

Hydrogen diffusivity in Fe-40 at.%Al alloy

Marian KUPKA^{1*}, Karol STĘPIEŃ¹

¹ Silesian University, Institute of Materials Science, Bankowa 12, 40-007 Katowice, Poland

* Corresponding author. Tel.: +48-32-259-6929; e-mail: marian.kupka@us.edu.pl

Received September 19, 2007; accepted November 11, 2008; available on-line March 19, 2009

Hydrogen diffusivity in iron aluminide (Fe-40 at.% Al) was studied using the electrochemical permeation technique at various cathode current densities. The effective diffusion coefficient was evaluated using the time-lag method. The changes in hydrogen diffusivity in the studied alloy were interpreted based on the observed changes in the charging conditions and the membrane structure.

Iron aluminides / Electrolytic charging / Hydrogen diffusivity

1. Introduction

Iron-aluminium alloys containing 22-50 at.% Al are a potential structural material for high-temperature applications. These materials show a high tendency to create a stable protecting layer of aluminium oxide, which provides perfect resistance to oxidation, carburisation and sulphurisation. The low density of the Fe-Al alloys and the price of their components are additional advantages of these materials. The main obstacle in the practical usage of iron aluminides is their low plasticity at room temperature due to internal weakness of grain boundaries, excess of thermal vacancies and environmental embrittlement [1].

The environmental embrittlement of iron aluminides results from the interaction of water vapour present in the air with aluminium. The mechanism of this interaction proposed by Liu, Lee and McKamey [2] is similar to the mechanism for aluminium and its alloys [3]. The brittleness is caused by the reduction of water vapour: $2Al + 3H_2O \rightarrow Al_2O_3 + 6H$, during which aluminium oxide and atomic hydrogen are created. Hydrogen, chemically adsorbed at the alloy surface, penetrates into the metal lattice and induces the classical hydrogen brittleness at crack tips, where new interfaces are created due to stress concentration.

The mechanism of the environmental embrittlement in Fe-Al alloys is not fully explained. Therefore, hydrogen transport in iron aluminides is one of the important factors that should be understood. Hydrogen permeation in metals and alloys is a complex phenomenon including several successive stages: adsorption, dissociation, dissolution, diffusion, recombination and desorption [4]. This process is influenced not only by the temperature, pressure or

metal layer thickness, but also by the value of forces of the gas interaction with metal, the metal structure, the ratio of the gas and metal atomic radii, the state of the metal surface and the charging conditions. From the point of view of hydrogen embrittlement of iron aluminides, the process of permeation of adsorbed hydrogen atoms to the inside of the metal and the diffusion inside the metal is most important.

The electrochemical permeation experiment introduced by Devanathan and Stachurski [5] is the method most commonly used to measure hydrogen diffusivity [6-9]. In this method, the entry side of a membrane made of the studied metal is in contact with a water solution of an electrolyte, from which hydrogen is released as a result of cathodic polarisation forced by an external source of current. A large part of the hydrogen usually escapes from the solution, but some of it penetrates into the membrane, migrates inside it and moves to the other (exit) side. To accelerate the departure of hydrogen from the membrane, it is subject to electrochemical ionisation (oxidation) in an alkaline solution at a constant, sufficiently high electrode potential of the exit side of the membrane [10]. The resulting ionisation current is a direct measure of the rate of hydrogen permeation through the membrane and it can be analysed in terms of hydrogen transport in the studied material [11]. The exit side of the membrane is covered with a thin layer of palladium. This layer should: - impede the reaction of the metal with the alkaline solution (anodic passivation), with which additional current flow and an apparent increase of the hydrogen penetration rate would be connected; - accelerate the electrochemical ionisation of hydrogen atoms and thereby making their chemical desorption – which would correspond to an apparent reduction of the permeation rate –

impossible. Electrochemical measurement of hydrogen diffusivity is not only convenient, but also extremely accurate. Changes in current density of $1 \cdot 10^{-3} \text{ A/m}^2$, which are easily measurable, correspond to changes in the stream of penetrating hydrogen of $1.04 \cdot 10^{-8} \text{ mole H/m}^2\text{s}$ [10].

Results of studies described by Barcik and Stępień [12] show that the choice of the electrolyte for cathode charging of iron aluminides with hydrogen may pose specific problems. The selected solution must be capable of destroying the surface Al_2O_3 layer. The oxide surface was found not only to decrease the hydrogen permeability to $1/2 \div 1/3$ of the value for the unoxidised specimen, but also to reduce the subsurface hydrogen concentration [7]. Results of investigations suggest that a 30% NaCl aqueous solution is the best electrolyte for iron aluminides.

Apart from the electrolyte type, the cathode current intensity is the second factor, which may significantly influence the cathode hydrogen permeation rate and hence the diffusion coefficient.

The present work aimed at investigating the effect of the cathode current intensity on the hydrogen permeation in iron aluminide membranes during electrolytic charging. Relatively high values of charging current were chosen to ensure that the Al_2O_3 layer, retarding hydrogen penetration, is removed from the entry surface of the membrane.

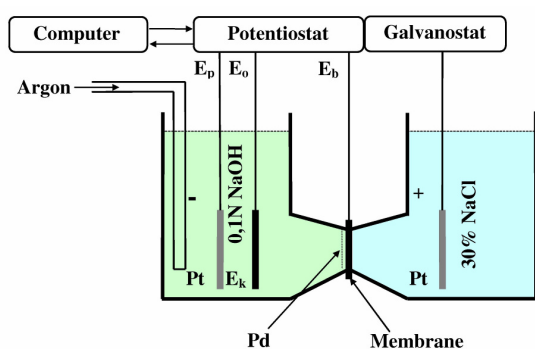


Fig. 1 Diagram of the apparatus used for the electrochemical investigation of hydrogen permeation through metal membranes: E_b – investigated electrode; E_p – auxiliary electrode; E_k – calomel electrode.

2. Experimental

The studies were carried out on a Fe-40 at.% Al alloy obtained by the technique of induction melting in vacuum according to the procedure described by Barcik *et al.* [13]. The obtained ingot, 20 mm in diameter and 70 mm long, was homogenised at $1000^\circ\text{C}/72\text{h}$ and then cooled in the furnace. It was cut into ca. 2.5 mm thick membranes. The surface of each membrane was ground, polished and degassed. A block diagram of the connections of the apparatus is

presented in Fig. 1. The membrane was mounted in a Teflon fixture between two electrolyzers. In the cell on the entry side of a membrane there was a 35 g NaCl/100 g H_2O solution educing hydrogen that was absorbed into the membrane and passed through the metal and was ionised in the exit cell. During hydrogen charging, the entry side of the membrane was the cathode, while a platinum electrode was the anode. On the exit side, the surface of the membrane covered with palladium was in constant contact with a 0.1N NaOH solution and was the anode, while a platinum electrode was the cathode. A calomel electrode was used as reference electrode, which through a potentiostat maintained the exit side of the membrane at a constant potential of +50 mV. This enabled the oxidation of hydrogen ($\text{H} - e \Rightarrow \text{H}^+$). Under the influence of electrons released from this reaction, a current of intensity i_p was flowing through the platinum electrode. The studies were carried out at the saturation current density $i_c = (2.55, 5.10, 9.55, 12.74, \text{ and } 19.11) \cdot 10^{-3} \text{ A/m}^2$. The measured intensity of the anode current, i_p , was proportional to the hydrogen permeation rate through the membrane. The measurements were carried out at room temperature. The permeation of hydrogen through the membrane was illustrated by curves of the permeation current i_p versus the saturation time t . The so called time-lag t_L can be determined as the time corresponding to the ratio $i_p/i_{pmax} = 0.617$; i_{pmax} is a steady state (maximum) permeation rate. The t_L may be used for calculating the effective diffusion coefficient D_{eff} of hydrogen using the equation :

$$D_{eff} = L^2/6t_L \quad (1)$$

[6-9,14], where L is the specimen (membrane) thickness. Three permeation tests were carried out for each value of the polarisation current intensity.

To perform qualitative phase analyses of the studied material, X-ray diffraction patterns were obtained using a PHILIPS diffractometer. Spectra were obtained using Cu $K\alpha$ radiation of 1.54178 \AA wavelength for the angle range $2\theta = 20\text{-}120^\circ$ with continuous recording.

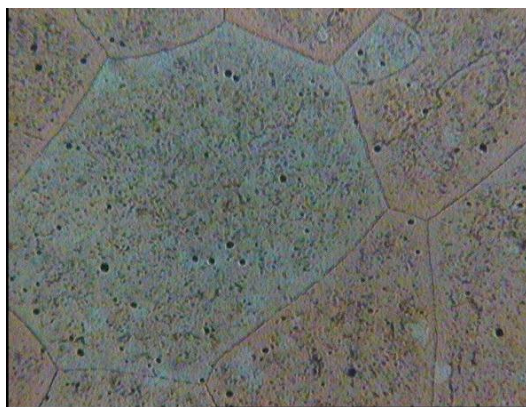


Fig. 2 Microstructure of the Fe-40 at.% Al alloy membrane after homogenisation (enlargement 100 \times).

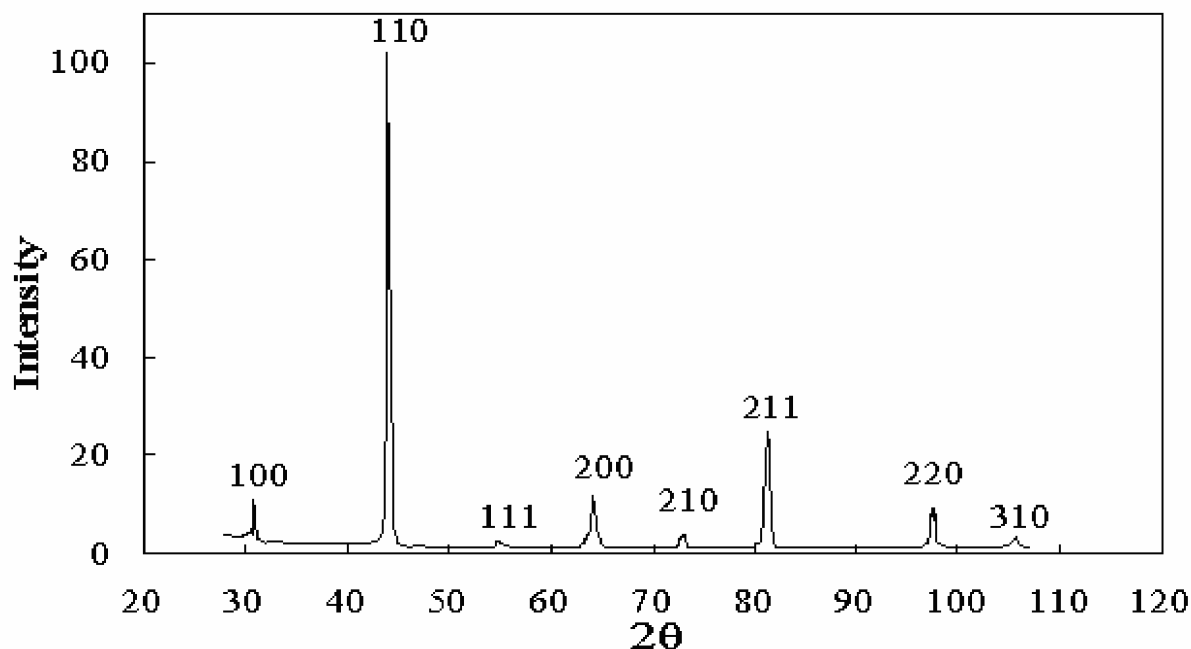


Fig. 3 X-ray diffraction pattern of the Fe-40 at.% Al alloy membrane after homogenisation.

The microstructure was examined using a light microscope NEOPHOT-2. The entry surface of the membrane after hydrogen charging was studied using a scanning electron microscope, while the chemical composition of the surface layer was determined using an EDS microanalyser.

3. Results and discussion

After homogenisation the studied alloy showed an equiaxed grain structure with an average grain size of $389 \pm 10 \mu\text{m}$ (Fig. 2). Eight reflections were registered during the X-ray phase analysis (Fig. 3). On the basis of the applied Rietveld procedure in which a theoretical diffraction pattern for the B2 phase was fitted to the diffraction pattern obtained from the experiment, the lattice parameter $a_0 = 2.89551 \text{ \AA}$ ($\Delta a_0 = 5.7 \cdot 10^{-5} \text{ \AA}$) was determined. A similar value of this parameter was also determined for the Fe-40 at.% Al phase in [15]. The obtained diffraction diagram agreed well with the data for the FeAl phase presented in the ASTM card file. The presence of lines for which the sum of hkl indices is an odd number proves that there is a long range order in the studied material. The comparison of the relative intensities of the experimental diffraction lines with the file data for the stoichiometric Fe₅₀Al₅₀ and off-stoichiometric Fe₆₀Al₄₀ phases shows a decrease in the superstructure line intensities with respect to the standards. This indicates that the degree of long range order in the studied alloy is low.

Based on the X-ray diffraction analysis the studied material was assumed to be a single-phase material of the B2 FeAl structure.

The permeation curves i_p versus t for a given value of the charging current density i_c were computer-registered (Fig. 4). Two types of permeation curve may be distinguished. For a lower cathode current density ($i_c = 2.55 \cdot 10^{-3}$ and $5.10 \cdot 10^{-3} \text{ A/m}^2$) the anode current increases in a parabolic way, reaches a plateau and maintains an approximately constant value up to long periods of hydrogen saturation. For a higher value of cathode current ($i_c = 9.55 \cdot 10^{-3}$, $12.74 \cdot 10^{-3}$, and $19.11 \cdot 10^{-3} \text{ A/m}^2$) the anode current increases up to a maximum and then clearly diminishes. The decrease in the anode current occurs after a shorter period of time and the stronger it is the higher is the cathode current density. As the cathode current density increases, the increase in the permeation rate is faster and the i_{pmax} value is larger. Fig. 5 shows the maximum penetration rate i_{pmax} versus the square root of the polarisation current density of the cathode i_c . The relationship is not linear and a few stages can be distinguished. The hydrogen permeation rate approximates a constant value starting from $i_c = 12.74 \cdot 10^{-3} \text{ A/m}^2$. A similar course of $i_p = f(i_c)^{1/2}$ was observed during studies on hydrogen permeation through iron membranes [4]. The range of d in Fig. 5 is particularly important, because only within this range the rate of hydrogen permeation is no longer dependant on surface phenomena occurring on the entry surface of the membrane. The experimental results are presented in a numerical form in Table 1. Also the calculated values of the effective hydrogen diffusion coefficient (D_{eff}) are shown. D_{eff} increases with increasing cathode polarisation current density. Based on the data presented in Fig. 5, it may be assumed that the value of $D_{eff} = 4.81 \cdot 10^{-10} \text{ m}^2/\text{s}$ is closest to the real effective hydrogen diffusion

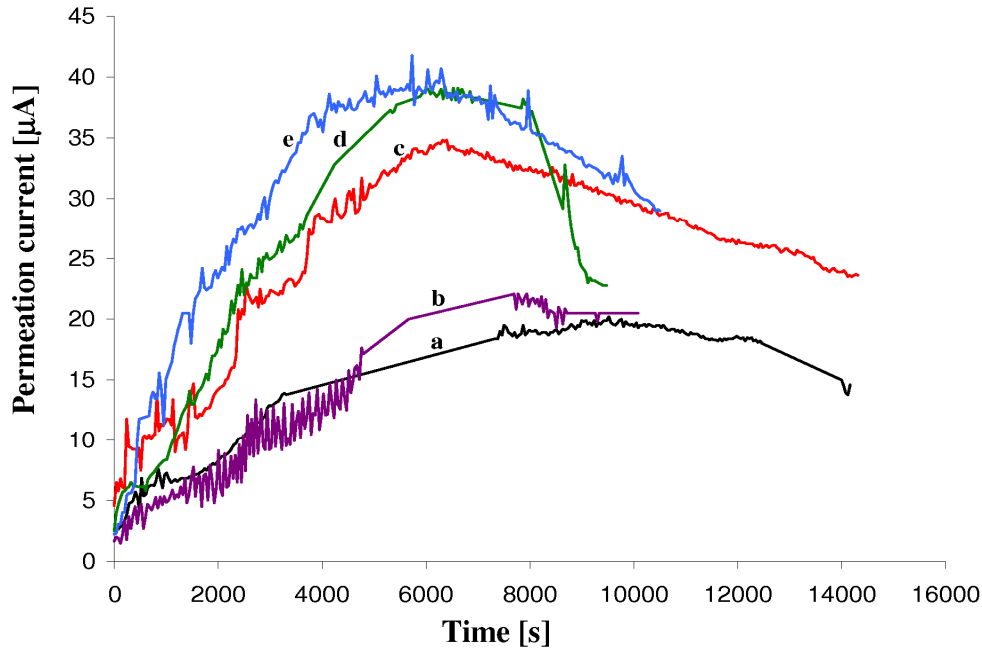


Fig. 4 The permeation curves for the Fe-40 at.% Al alloy at different values of cathode polarisation current density : a – $i_c = 2.55 \cdot 10^{-3} \text{ A/m}^2$, b – $i_c = 5.10 \cdot 10^{-3} \text{ A/m}^2$, c – $i_c = 9.55 \cdot 10^{-3} \text{ A/m}^2$, d – $i_c = 12.74 \cdot 10^{-3} \text{ A/m}^2$, e – $i_c = 19.11 \cdot 10^{-3} \text{ A/m}^2$.

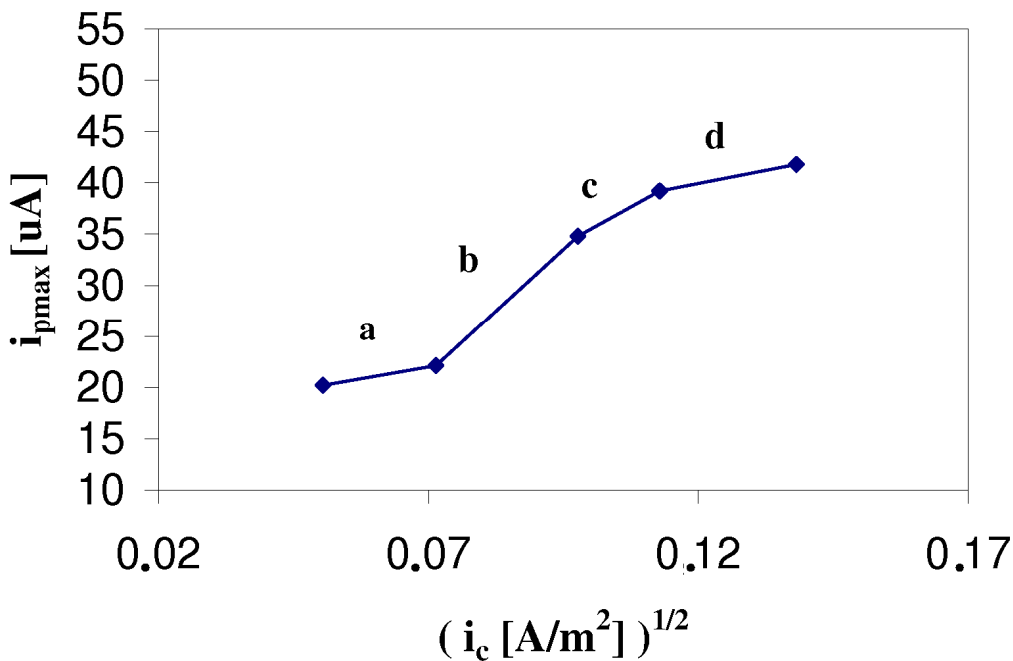


Fig. 5 Maximum value of current intensity i_{pmax} versus square root of cathode polarisation current density i_c for the Fe-40 at.% Al alloy.

coefficient in Fe-40 at.% Al. The hydrogen diffusivity in pure iron, calculated from reliable data at 300 K, is about $10^{-8} \text{ m}^2/\text{s}$ [16]. Knowledge of the diffusion in the intermetallic phase B2 FeAl is sparse [17]. The values of the hydrogen diffusion coefficient obtained in [17] and in the present work are in the order of $10^{-10} \text{ m}^2/\text{s}$. So it may be concluded that the introduction of aluminium into αFe reduces the hydrogen diffusion rate. Similar results were obtained in [16] and [18] for

Fe_3Al alloys. Banerjee and Balasubramaniam [16] attributed the lower hydrogen diffusivity in the iron aluminide containing higher amounts of Al to the trapping tendency of Al. According to Hosoda *et al.* [18], Al atoms play the role of repellers due to their strong repulsive force to hydrogen. The repeller reduces the effective diffusion path so that the total diffusivity is lowered with increasing concentration of repeller elements. In B2 FeAl alloys, the value of the

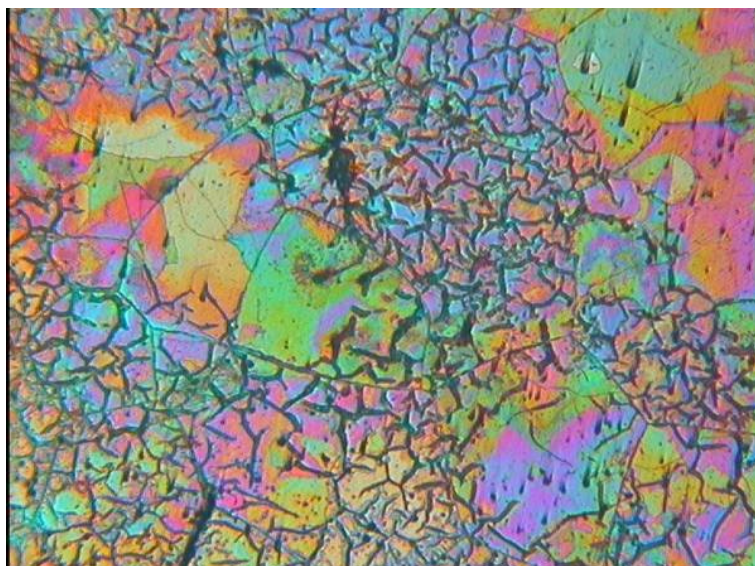


Fig. 6 Microscope image of the Fe-40 at.% Al alloy membrane surface on the hydrogen penetration side after 3-hour hydrogen charging at a cathode current density of $9.55 \cdot 10^{-3} \text{ A/m}^2$ (enlargement 100×).

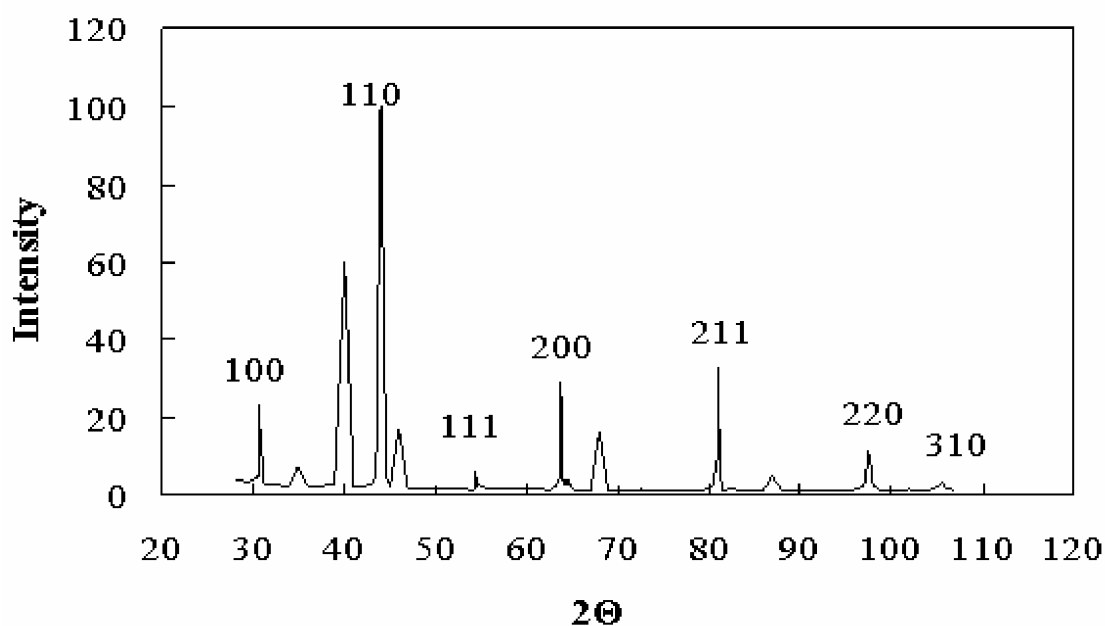


Fig. 7 X-ray diffraction pattern of the Fe-40 at.% Al alloy membrane after hydrogen charging ($i_c = 9.55 \cdot 10^{-3} \text{ A/m}^2$, $t = 3 \text{ h}$).

hydrogen diffusion coefficient falls with increasing aluminium content, thereby indicating that increasing amounts of Al addition lower the hydrogen diffusivity [17]. The lack of diffusion coefficient dependence on the grain size indicates that the hydrogen transport through the B2 FeAl phase mainly occurs via bulk diffusion, through interstices in the crystal lattice [17]. The observed increase in microhardness as a result of hydrogen charging of B2 iron aluminides is the effect of solution hardening caused by the presence of hydrogen atoms occupying interstices in the alloy lattice [19].

Studies of the microstructure of the membrane after hydrogen charging, at the stage of clear decrease

in the anode current intensity, have shown that its surface on the entry side is covered with corrosion products created as a result of the influence of the electrolyte (Fig. 6).

Fig. 7 presents an X-ray diffraction pattern from the surface of the material studied after hydrogen charging. Apart from lines originating from the Fe-40 at.% Al phase, lines from the corrosion products are visible, the relative intensity of which reach 1/3 of the line intensity of the basic phase. It has been found that iron chloride is the corrosion product. To confirm this, the entry surface of the membrane was observed using a scanning electron microscope (Fig. 8) and the element content in the corrosion product was

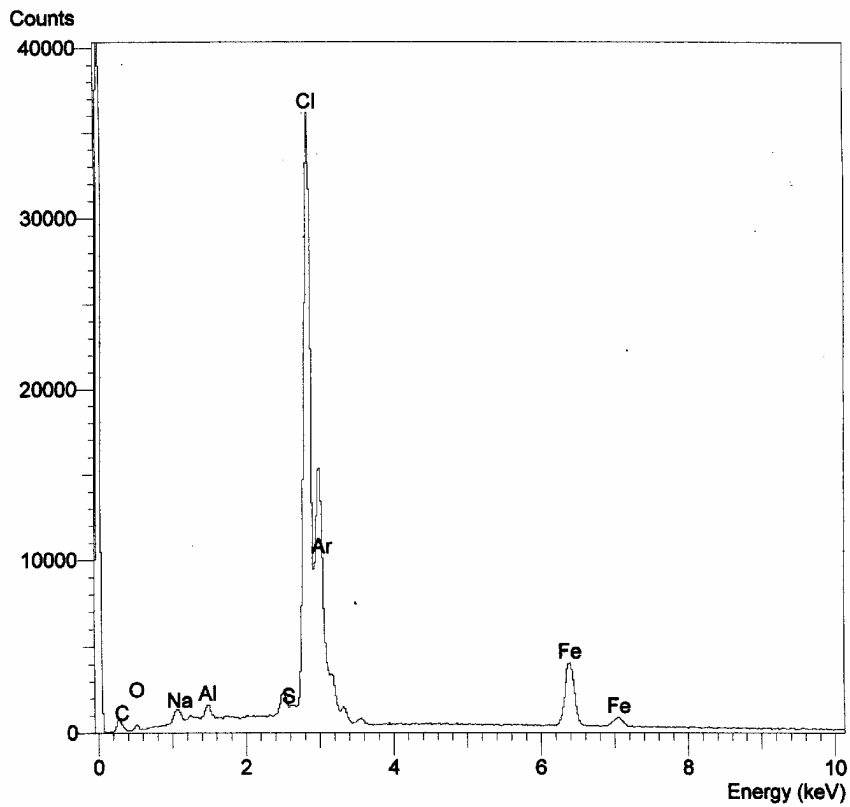
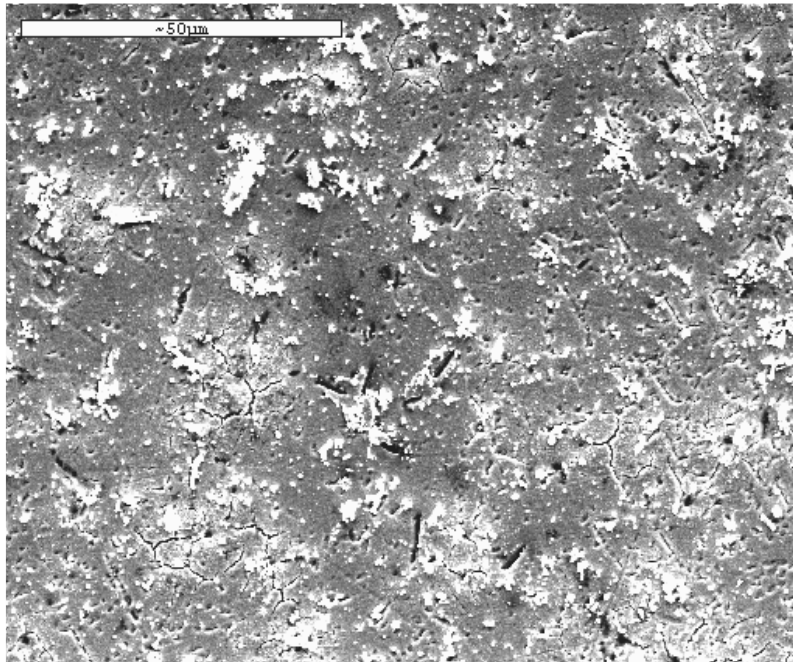


Fig. 8 Image of the surface of a hydrogen charged membrane and the result of the linear chemical analysis of the corrosion products (SEM micrograph).

determined (Fig. 9). The results obtained confirmed the results of the X-ray phase analysis that FeCl_3 is the only surface corrosion product. The presence of lines occurring for argon in the spectra shown in Fig. 8 and Fig. 9 can be explained by the fact that during the

measurement, the sample surface was kept under argon atmosphere. The formation of an iron chloride layer on the membrane surface on the hydrogen penetration side for cathode polarisation current densities exceeding $5 \cdot 10^{-3} \text{ A/m}^2$, was certainly the

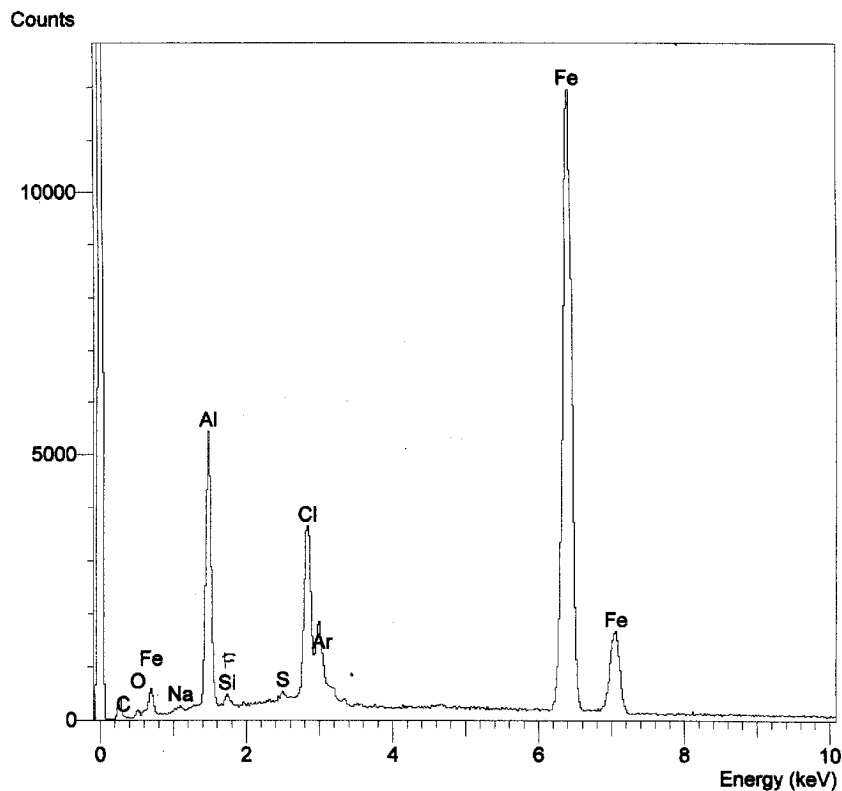
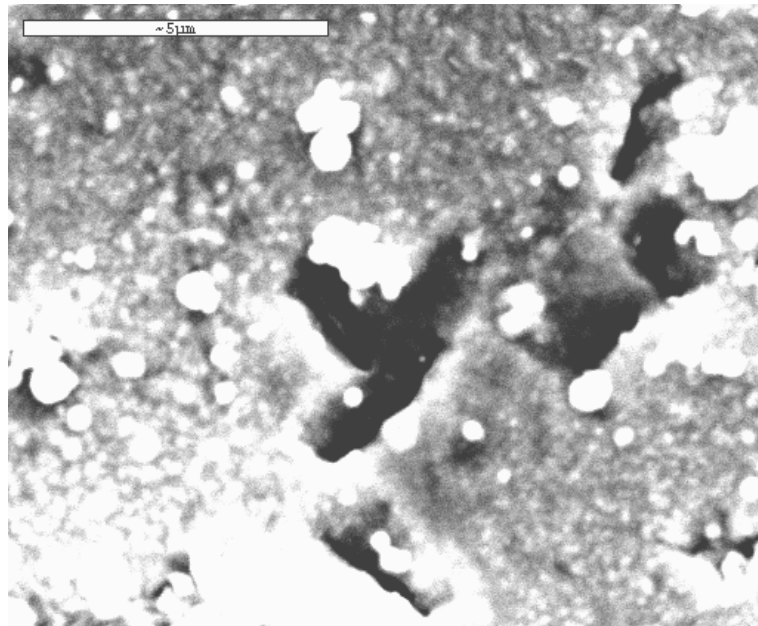


Fig. 9 Chemical composition of the surface layer of the Fe-40 at.% Al membrane after hydrogen charging (EDS scan).

reason for the decrease of the anode current (hydrogen permeation rate) after reaching the maximum value (Fig. 4).

4. Conclusions

The electrolytic method of cathode charging is very useful to study hydrogen diffusivity in iron

aluminides. The selection of appropriate electrolysis conditions – electrolyte composition and charging current density – is the condition for the effectiveness of the method and for the reliability of the obtained results. In this study a 35% aqueous solution of NaCl was used, the composition being selected based on results of studies presented in [12], where it was found that this electrolyte is able to remove the blocking oxide layer (Al_2O_3) to a sufficient extent for free

hydrogen penetration into the FeAl alloy. The present studies have shown that to remove such a layer the cathode current density must be sufficiently high (at least around $12.74 \cdot 10^{-3}$ A/m²). At this saturation current density the values of the effective hydrogen diffusivity calculated using the method of “time-lag” are reliable. After longer time of hydrogen charging the entry surface of the membrane made of Fe-40 at.% Al was covered with a layer of iron chloride, which caused a reduction of the hydrogen permeation rate. As the “time-lag” is determined based on the rising part of the permeation curve, the creation of this blocking layer does not affect the precision of D_{eff} .

References

- [1] L.M. Pike, C.T. Liu, *Scr. Mater.* 38 (1998) 1475.
- [2] C.T. Liu, E.H. Lee, C.G. McKamey, *Scr. Metall.* 23 (1989) 875.
- [3] V.K. Sikka, S. Viswanathan, C.G. McKamey, In: R. Darolia, J.J. Lewandowski, C.T. Liu, P.L. Martin, D.B. Miracle, M.V. Nathal (Eds.), *Structural Intermetallics*, The Minerals, Metals & Materials Society, 1993, p. 483.
- [4] M. Śmiałowski, *Wodór w stali (Hydrogen in Steel)*, WNT, Warsaw, 1961, p. 64.
- [5] M.A.V. Devanathan, Z. Stachurski, *Proc. R. Soc. A* 270 (1962) 90.
- [6] H. Chiu, L. Qiao, X. Mao, *Scr. Mater.* 34 (1996) 963.
- [7] W.C. Luu, J.K. Wu, *Corros. Science* 43 (2001) 2325.
- [8] B.H. Lim, H.S. Hong, K.S. Lee, *J. Nucl. Mater.* 312 (2003) 134.
- [9] H. Addach, P. Bercot, M. Rezzazi, M. Wery, *Mater. Lett.* 59 (2005) 1347.
- [10] T. Zakroczyński, *Wnikanie i transport wodoru w żelazie i jego stopach*, Polska Akademia Nauk, Instytut Chemii Fizycznej, Warszawa, 1990, p. 5.
- [11] T. Zakroczyński, *Proc. Int. Conf. Sci. & Econ.*, Warsaw, 2005, p. 151.
- [12] J. Barcik, K. Stępień, *Mater. Sci. Eng. A* 334 (2002) 28.
- [13] J. Barcik, A. Gierek, M. Kupka, T. Mikuszewski, T. Prandzioch, K. Stępień, *Hutn. Wiad. Hum.* 6 (2001) 214.
- [14] J. Crank, *The Mathematics of Diffusion*, Oxford University Press, Oxford, 1979, p. 51.
- [15] Y.A. Chang, L.M. Pike, C.T. Liu, A.R. Bilbrey, D.S. Stone, *Intermetallics* 1 (1993) 107.
- [16] P. Banerjee, R. Balasubramaniam, *Scr. Mater.* 39 (1998) 1215.
- [17] K. Stępień, M. Kupka, *Scr. Mater.* 55 (2006) 585.
- [18] H. Hosoda, K. Yoshimi, K. Inoue, S. Hanada, *Mater. Sci. Eng. A* 258 (1998) 135.
- [19] K. Stępień, M. Kupka, *Scr. Mater.* 59 (2008) 999.

Proceeding of the X International Conference on Crystal Chemistry of Intermetallic Compounds, Lviv, September 17-20, 2007.